

Ultracold atoms in optical lattices: tunable quantum many-body systems

W. HOFSTETTER*

Institut fuer Theoretische Physik A, RWTH Aachen,
Templergraben 55, 52056 Aachen, Germany

(Received 16 February 2005; in final form 30 May 2005)

Cold atoms in optical lattices offer an exciting new laboratory where quantum many-body phenomena can be realized in a highly controlled way. They can even serve as *quantum simulators* for notoriously difficult problems like high-temperature superconductivity. This review is focussed on the recent developments and new results in multi-component systems. Fermionic atoms with SU(N) symmetry have exotic superfluid and flavor-ordered ground states. We discuss symmetry breaking, collective modes, and detection issues, e.g. in Bragg scattering. On the other hand, bosonic multiflavor ensembles allow for engineering of spin Hamiltonians which are interesting from a quantum computation point of view. Finally, we address the role of disorder in optical lattices. Fermionic atoms experience Anderson localization at sufficiently strong disorder. Interactions among the atoms induce a competing tendency towards delocalization. We present a complete phase diagram obtained within dynamical mean-field theory and discuss experimental observability of the Mott and Anderson phases.

1. Introduction and overview

The achievement of Bose–Einstein condensation (BEC) 10 years ago [1–3] has pioneered the new field of interacting quantum gases in the dilute limit. It has become possible for the first time to observe quantum phenomena like Bose statistics on a mesoscopic scale, involving a large number of atoms. More recently, also fermionic gases have been cooled to the quantum degenerate regime, using sympathetic cooling of two spin states or boson–fermion mixtures [4–7]. Although the resulting temperatures $T/T_F \approx 0.1$ are, relative to the Fermi temperature T_F , much higher than in solids, the Pauli principle has been clearly observed. In addition to quantum statistics, tunable interactions are another important ingredient in the cold atom ‘toolbox’. The interactions between atoms can be changed by an external magnetic field as a result of Feshbach resonance [8, 9]. In particular, their scattering length can be tuned to positive or negative values, corresponding to repulsive or attractive interactions. This has opened the way to studies of solid-state related phenomena like

*Email: hofstett@physik.rwth-aachen.de

Cooper pairing and, BCS superfluidity of fermions [10, 11]. The resulting BEC–BCS crossover has recently been the subject of intense experimental and theoretical studies [12–14].

In an independent development, degenerate atomic clouds have been combined with optical lattices, created by standing light waves which generate an effective periodic potential for the atoms [15–17]. This way interactions can be tuned without changing the atomic scattering length. This has been demonstrated in a pathbreaking experiment [15] where interacting bosons were tuned through a quantum phase transition from a superfluid (SF) to a Mott insulating state. Very recently, fermionic K^{40} atoms have been loaded into 3d optical lattices as well [18]. In these new experiments the lowest Bloch band was filled up successively, and the shape of the Fermi surface monitored by time-of-flight measurements. Eventually, a completely filled Brillouin zone corresponding to a band insulator was observed.

More generally, fermionic atoms in optical lattices allow for the realization of solid-state type quantum phases like antiferromagnetism or high-temperature superconductivity [19]. Even the spatial dimensionality of the lattice can be tuned. As an example, one-dimensional optical lattices have been realized where the hardcore or Tonks-gas limit of interacting bosons has been observed [20, 21]. Recent progress in numerical methods for simulating 1d quantum systems has lead to interesting predictions about the dynamics of such systems [22, 23].

In the following we shall first give an overview of the basic models describing cold atoms in optical lattices, together with a discussion of solid-state related phenomena which can be observed. We will then address systems with multiple flavors, i.e. hyperfine states, which allow realization of new exotic quantum states not accessible in solids. Finally, we discuss the role of disorder in current and future experiments involving cold atoms.

2. Optical lattices and strong correlations

2.1. Model and parameters

Atoms can be trapped in standing light waves created by interfering laser beams detuned far from resonance [15–17]. Due to the AC Stark shift the atoms experience a periodic potential of the form

$$V(x) = V_0 \sum_{i=1,2,3} \cos^2(kx_i) \quad (1)$$

where k is the wave vector of the laser. The natural energy scale for the potential depth V_0 is the *recoil energy* $E_R = \hbar^2 k^2 / 2m$. A schematic picture of such an optical lattice is shown in figure 1. The translational eigenstates in the periodic lattice potential are given by Bloch bands. An equivalent representation in terms of Wannier orbitals leads to tight-binding Hamiltonian. Let us assume for the moment that two different (hyperfine-) spin states are present, which in the following are denoted as $\sigma = \uparrow, \downarrow$. If temperature and filling are sufficiently low, the atoms will be confined exclusively to the lowest Bloch band. In this case the system can be

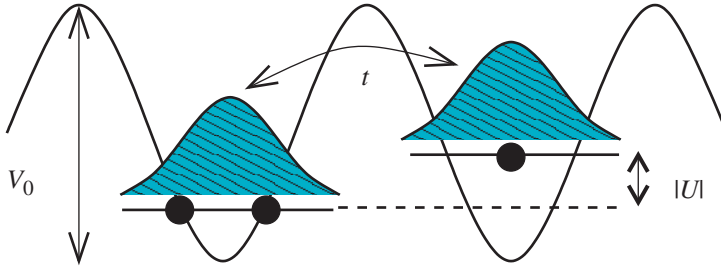


Figure 1. Cold atoms in an optical lattice of strength V_0 , shown here with hopping t and negative onsite interaction U . This situation corresponds to an attractive Hubbard model where multiple occupancy of lattice sites is energetically favorable.

described by a Hubbard Hamiltonian [24–26]

$$H = -t \sum_{\langle ij \rangle, \sigma} (c_{i\sigma}^\dagger c_{j\sigma} + c_{j\sigma}^\dagger c_{i\sigma}) + U \sum_i n_{i\uparrow} n_{i\downarrow} \quad (2)$$

where $c_{i\sigma}$ is the fermionic annihilation operator for the Wannier state of spin σ on site i and $n_{i\sigma} = c_{i\sigma}^\dagger c_{i\sigma}$ is the corresponding number density. Let $\Psi(\mathbf{x} - \mathbf{x}_i)$ be a single Wannier function localized at the i th lattice site. The parameters for hopping t and onsite interaction U can then be expressed in terms of overlap integrals as

$$t = - \int d^3x \Psi(\mathbf{x} - \mathbf{x}_i) \left(-\frac{\hbar^2 \nabla^2}{2m} + V_{\text{lattice}}(\mathbf{x}) \right) \Psi(\mathbf{x} - \mathbf{x}_j) \quad (3)$$

$$U = \frac{4\pi\hbar^2 a_s}{m} \int d^3x |\Psi(\mathbf{x})|^4$$

with the final result

$$t = E_R (2/\sqrt{\pi}) \xi^3 \exp(-2\xi^2) \quad (4)$$

$$U = E_R a_s k \sqrt{8/\pi} \xi^3$$

where a_s is the atomic scattering length and $\xi = (V_0/E)^{1/4}$ is a parameter characterizing the strength of the lattice [16, 19]. From equation (4) it is obvious that by tuning the optical lattice potential V_0 one can achieve arbitrary ratios $|U|/t$ without changing a_s . Optical lattices thus give access to the *strongly correlated* regime without using Feshbach resonances, which can entail problems of their own like enhanced losses or instabilities.

2.2. Superfluid-insulator transition

These highly controllable interactions have been employed to study the transition from a Bose condensate of Rb^{87} atoms with weak repulsive interactions to a Mott insulator [15]. In this experiment only a single hyperfine state was used, i.e. the appropriate theoretical description of the results involves a spinless bosonic

Hubbard model. For weak interactions, where the kinetic energy dominates, the atoms are delocalized across the entire lattice and the superfluid many-body ground state can be written approximately as

$$|\Psi_{\text{SF}}\rangle \sim \left(\sum_{i=1}^N b_i^\dagger \right)^N |0\rangle \quad (5)$$

where $|0\rangle$ is the empty lattice and N the number of lattice sites. Here all bosons have condensed into the same Bloch state with lattice momentum $k=0$. Note that in this state the probability distribution for the local occupation n_i is poissonian. If, on the other hand, the onsite repulsion U dominates, fluctuations in the local occupation number become energetically unfavorable. At commensurate filling of n atoms per site the ground state can be written as a product of local Fock states:

$$|\Psi_{\text{Mott}}\rangle \sim \prod_{i=1}^N (b_i^\dagger)^n |0\rangle. \quad (6)$$

This Mott state is incompressible and unlike the superfluid cannot be described by a macroscopic wave function. In the experiment by Greiner *et al.* [15] the system was reversibly tuned between these two ground states by changing the strength V_0 of the optical lattice via the laser intensity. The momentum distribution of the atoms was measured by a time-of-flight technique and clearly showed the loss of coherent tunneling in the Mott insulator. In this experiment it has thus been demonstrated that optical lattices are an ideal tool for analyzing quantum phase transitions.

2.3. High-temperature fermionic superfluidity

In this section we discuss a proposal for achieving superfluidity of fermionic spin 1/2 atoms in an optical lattice. Let us first focus on the situation with *attractive* interactions $U < 0$, where we expect *s*-wave pairing and condensation of Cooper pairs below a critical temperature T_c . According to BCS theory, for weakly confining atom traps the transition temperature scales exponentially with interaction strength $k_B T_c^{\text{free}} \approx 0.3 E_F^{\text{free}} \exp[-\pi/(2k_F |a_s|)]$ where E_F^{free} is the Fermi energy in the harmonic trap. This critical temperature is exceedingly low, unless the characteristic parameter $k_F |a_s|$ is increased to values of order unity by a Feshbach resonance. This has indeed been achieved in a remarkable series of recent experiments [12–14]. However, interpretation of the resulting BEC–BCS crossover is somewhat complicated due to mixing of multiple scattering channels at resonance.

In [19] we have suggested an alternative approach, which makes use of the tunable atomic interactions in an optical lattice, as sketched in figure 2. In the weak-tunneling limit $t \ll |U|$ of the negative U Hubbard model (2) one recovers the standard BCS picture with the exponentially small gap. However, increasing the optical lattice depth leads to both reduced tunneling t and enhanced interaction $|U|$. The result is a dramatically increased transition temperature T_c which can be pushed to a value of the order t^2/U , see figure 2. It is maximal in the crossover regime where interaction and kinetic energy are comparable [27].

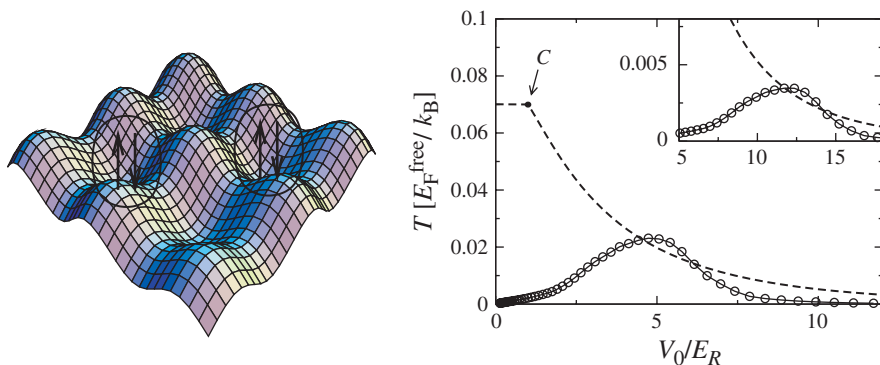


Figure 2. Left: Fermions with attractive interaction forming Cooper pairs in an optical lattice. Right: Critical temperature for the SF transition of Li^6 atoms as a function of the optical lattice depth in a 3d CO_2 lattice. Inset: analogous plot for K^{40} atoms in a Nd:YAG lattice. The dashed curves show the effect of an adiabatic cooling if the atoms are loaded into a weak lattice at point C which is then decoupled from the reservoir. Figures taken from [19].

We have additionally taken into account an *adiabatic cooling* effect for fermions in an optical lattice: if the atoms are filled into a weak lattice, which is then adiabatically switched on, the Bloch momentum will be approximately conserved, while the dispersion changes. As a result, the effective temperature of the fermions is lowered (see figure 2). Taking the cooling into account leads to a *universal* transition temperature $T_c^{\text{free}} \approx 0.1 E_F^{\text{free}}$ which has to be achieved before the gas is loaded into the lattice. Note that T_c^{free} is independent of the atom type and well within reach of today's experiments.

An even more intriguing possibility opens up for *repulsive* interactions $U > 0$ resulting from a positive scattering length $a_s > 0$. At half filling $n_i = 1$ this gives rise to staggered antiferromagnetic order. At lower filling fractions, on the other hand, cold fermions in a lattice could be used to experimentally probe *d-wave* pairing (see figure 3) in the 2d Hubbard model, which is currently beyond the limits of classical computing. The resulting superfluid order can be detected via Bragg scattering, which is by now a well-established technique, to measure the dynamical density response $S(q, \omega)$ in interacting quantum gases [28, 29].

Such *quantum simulations* along the lines of Feynman [30] could provide a powerful tool to gain insight into the many-body Hamiltonians relevant for solid-state physics.

3. Multi-component systems

3.1. Two-component bosons with spin order

All of the alkali atoms available for trapping and cooling have $2 \times (2I + 1)$ low-lying hyperfine states, where I is the nuclear spin. The three common bosonic isotopes Li^7 , Na^{23} and Rb^{87} all have the same value $I = 3/2$. Several of these states can be trapped at the same time: in magnetic traps one is limited by the condition that the states have to be *low-field seekers*, but optical dipole traps, created with a focussed

red-detuned laser beam, allow confinement of basically any combination of spin states [31], as long as no instability due to three-body collision occurs.

This is also true for optical lattices which, like optical traps, are based on the AC Stark effect. Loading a lattice with two hyperfine states of Rb⁸⁷ has been demonstrated experimentally in [32] where also a spin-dependent periodic potential has been implemented. In the following we discuss a proposal, first published in [33], how these techniques can be used to engineer quantum spin Hamiltonians which in turn could be relevant for quantum information processing.

Let us consider a system of two bosonic hyperfine states in a lattice, described by the following Bose–Hubbard Hamiltonian:

$$H = -t_a \sum_{\langle ij \rangle} (a_i^\dagger a_j + H.c.) - t_b \sum_{\langle ij \rangle} (b_i^\dagger b_j + h.c.) + U \sum_i \left(n_{ai} - \frac{1}{2} \right) \left(n_{bi} - \frac{1}{2} \right) + \frac{1}{2} \sum_{i, \alpha=a,b} V_\alpha n_{\alpha i} (n_{\alpha i} - 1) - \sum_{i, \alpha} \mu_\alpha n_{\alpha i}. \quad (7)$$

Here a_i, b_i denote the annihilation operators for two different bosonic pseudospin states, and the number operators are defined as $n_{ai} = a_i^\dagger a_i$, $n_{bi} = b_i^\dagger b_i$, with the corresponding chemical potentials $\mu_{\alpha(b)}$. In reality, experiments are performed at a fixed number of particles (i.e. fixed magnetization), which in the grand canonical description can be achieved by tuning the chemical potential. The onsite interaction between equal spin states is given by $V_{\alpha(b)}$, and the one between different spins by U . We also assume a spin-dependent tunable hopping $t_{\alpha(b)}$ which has already been experimentally realized [32].

We now focus on the case of integer filling $n_a + n_b = 1$, following [33]. We are mainly interested in the nature of the Mott–superfluid (SF) transition in this system, and the possibility of spin order in the insulating phase. To address the second issue, it is instructive to consider parameters $t_{\alpha,b} \ll U, V_{\alpha,b}$ deep inside the Mott phase. States with double occupancy per site are then very unfavorable and can be projected out by a Schrieffer–Wolff transformation. This leads to an effective spin Hamiltonian in the subspace of single occupation [34]

$$H_{\text{eff}} = J_z \sum_{\langle ij \rangle} S_i^z S_j^z - J_\perp \sum_{\langle ij \rangle} (S_i^x S_j^x + S_i^y S_j^y) - h \sum_i S_i^z \quad (8)$$

where spin labels \uparrow (\downarrow) denote sites occupied by a (b) atoms. The effective parameters are given by

$$J_z = 2 \frac{t_b^2 + t_a^2}{U} - \frac{4t_a^2}{V_a} - \frac{4t_b^2}{V_b} \\ J_\perp = \frac{4t_a t_b}{U} \\ h = \frac{2t_a^2}{V_a} - \frac{2t_b^2}{V_b} + h_{\text{ext}}. \quad (9)$$

We assume that the induced ordering field h can be cancelled by an external field h_{ext} . The physics of this XXZ model is well understood and includes an x – y ferromagnetic

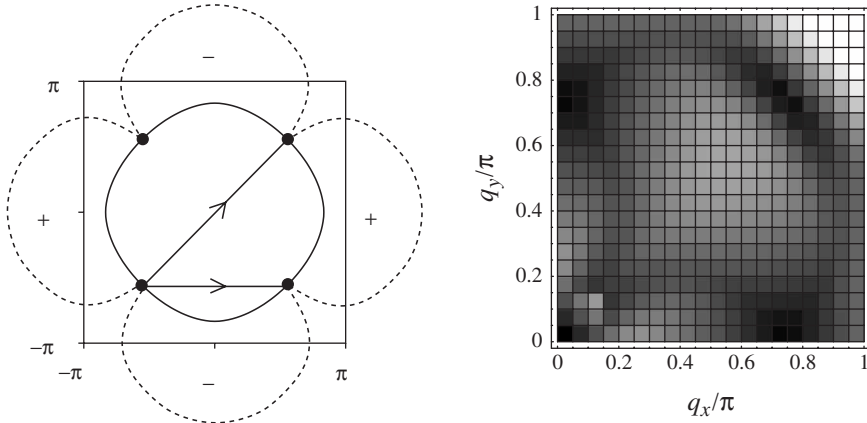


Figure 3. Probing d -wave pairing in the repulsive 2d Hubbard model via Bragg scattering. Left: schematic diagram of the Fermi surface in 2d (solid line) and the momentum dependence of the gap (dashed line). Right: onset frequency of the quasiparticle continuum in the dynamical structure factor $S(q, \omega)$, plotted as a function of momentum q . At the special wave vectors connecting the nodal points in the left figure, the density response is gapless. Figures taken from [19].

phase for $J_{\perp} > J_z > 0$ as well as an antiferromagnetic z -Neel ordered state for $J_z > J_{\perp} > 0$.

The disadvantage of this deep Mott regime is that the critical temperature for magnetic ordering is very low $T_c \sim \max(t_{a(b)}^2/U, t_{a(b)}^2/V_{a(b)})$ and therefore experimentally hardly accessible. In order to enhance T_c and study the region close to the Mott–SF transition it is necessary to make at least one of the interaction parameters comparable to the hopping. Here we choose $t_{a(b)} \approx U \ll V_{a(b)}$, which means that double occupancy with two different spins is now possible. The main question is whether the spin order discussed above is still visible close to the superfluid. In order to map out the Mott–SF phase boundary, we have used a mean-field approach first proposed by Sheshadri *et al.* [35] where the kinetic energy is decoupled:

$$\begin{aligned}
 H_{\text{MF}} = & U \sum_i \left(n_{ai} - \frac{1}{2} \right) \left(n_{bi} - \frac{1}{2} \right) + \frac{1}{2} \sum_{i; \alpha=a,b} V_{\alpha} n_{\alpha i} (n_{\alpha i} - 1) \\
 & - \sum_{\langle ij \rangle} t_a \left(a_i^{\dagger} \langle a_j \rangle + Hc \right) - t_b \sum_{\langle ij \rangle} \left(b_i^{\dagger} \langle b_j \rangle + h.c. \right) + \text{constant} \quad (10)
 \end{aligned}$$

In the paramagnetic phase, this decoupling leads to a sum of identical single-site Hamiltonians. We have solved the resulting self-consistency problem numerically, allowing for up to $M=9$ bosons per spin and sites. The phase diagram obtained in this way is shown in figure 4 (left). Note that as $V_{a(b)}$ decreases, the Mott domain shrinks.

Within the mean-field approach, different spin ordered states in the insulator cannot be resolved. In order to remove this degeneracy, it is necessary to take into account quantum fluctuations on top of the variational mean-field state and

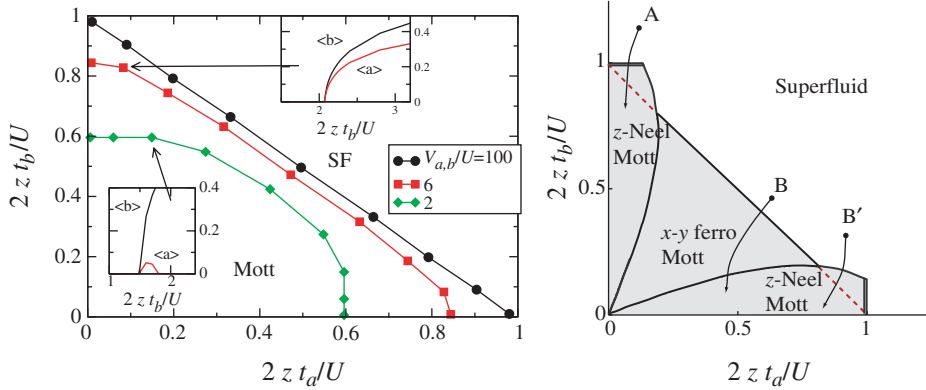


Figure 4. Left: Phase diagram of the 2-component bosonic Hubbard model obtained via decoupling mean-field theory. Note that as $V_{a(b)}$ decreases, the Mott domain shrinks. Right: Phase diagram including quantum fluctuations. Figures taken from [33].

compare the resulting ground state energies. Details of this calculation can be found in [33]. The resulting phase diagram including fluctuations is given in figure 4 (right). Spin ordering persists right up to the SF phase boundary and can, furthermore, be tuned from xy -ferromagnetic to z -Neel antiferromagnetic by the ratio t_a/t_b . We find hysteresis between the z -Neel state and the superfluid, while the transition between the xy -state and the SF is continuous. These should be a clear signature for an experimental detection of spin ordered states, using for example Rb^{87} atoms. The spin order can be directly observed using spin-dependent Bragg scattering or via density fluctuation in time-of-flight measurements [36].

3.2. Beyond solid-state: $SU(N)$ fermions

As discussed in section 2.3, fermionic atoms in optical lattices can be used to perform quantum simulations of complex solid-state systems like the cuprate superconductors. Now we show that with the degrees of freedom offered by ultracold atoms, it is also possible to create new states of matter that have no equivalent in condensed matter at all. The obvious constraint in solid-state physics is that electrons have only two spin states. Atoms, on the other hand, have large hyperfine multiplets out of which several states can be trapped simultaneously. For fermionic atom this has been demonstrated with the three states $|F = 9/2, m_F = -5/2, -7/2, -9/2\rangle$ of K^{40} in an optical trap [37]. Alternatively, one could use the three spin polarized $m_s = 1/2$ states of Li^6 which, in a sufficiently large field, have a pairwise equal and anomalously large triplet scattering length $a_s = -2160a_0$ [38].

These systems can be used to realize fermionic Hubbard models with $N > 2$ flavors and approximate $SU(N)$ flavor symmetry. In the following we discuss the rich physics of these models for finite N , following the work by Honerkamp and Hofstetter [39, 40]. The Hamiltonian is given by

$$H = -t \sum_{m, \langle ij \rangle} [c_{i,m}^\dagger c_{j,m} + c_{j,m}^\dagger c_{i,m}] + \frac{U}{2} \sum_i n_i^2 \quad (11)$$

where c_{im}^\dagger creates a fermion of flavor $m = 1, \dots, N$ on site i and $n_i = \sum_m n_{i,m}$ is the total number of atoms on site i . Note that the interaction term has local $SU(N)$ invariance while the hopping reduces this to a global one. The values of t and U can be derived from atomic parameters along the lines of section 2.1.

While the large- N limit of this model has been well studied in the context of high- T_c superconductivity [41], few results have been previously obtained for finite N . Consider first the case of repulsive interactions $U > 0$. We have performed a systematic analysis of weak-coupling instabilities using a perturbative functional renormalization group (RG) approach [42]. In this technique, the 2-body interaction is parametrized by a coupling function $V(k_1, k_2, k_3)$, the flow of which is monitored as a function of some cutoff parameter like the temperature T . In this way one can identify singular response e.g. in the charge channel or in the $SU(N)$ channel. Although the RG eventually breaks down at strong coupling, it allows to identify the leading instability towards an ordered phase. The analysis performed by Honerkamp and Hofstetter [39] focuses on $d=2$ dimensions.

In figure 5 the three relevant types of order at half filling $\langle n_i \rangle = N/2$ are shown. In the spin 1/2 case the system displays staggered antiferromagnetic order, as is well known. For intermediate $N < 6$ the RG yields an instability towards flavor density wave states with ordering wavevector $\mathbf{Q} = (\pi, \pi)$ like in the antiferromagnetic case. This corresponds to a breaking of the $SU(N)$ symmetry, leading to a degenerate ground state manifold. As N increases, breaking of $SU(N)$ becomes less favorable because the number of Goldstone modes increases. For $N > 6$ the RG indicates a dominant instability of the *staggered flux* type with alternating particle currents around the plaquettes of the 2d lattice (see figure 5c). This state breaks only translational and time-reversal invariance and has a finite expectation value of the d -wave density component $\Phi_{SF} = \sum_{\vec{k}, m} (\cos k_x - \cos k_y) \langle c_{\vec{k}, m}^\dagger c_{\vec{k}+\vec{Q}, m} \rangle$, again with ordering wavevector $\mathbf{Q} = (\pi, \pi)$.

Let us briefly discuss the temperature scales T_c below which the respective long-range orders set in. The critical temperature for flavor density wave order at strong coupling scales like t^2/U and can thus be tuned to relatively large values: for $N=3$ the RG predicts a maximum T_c of $\approx 0.1 t$. On the other hand, staggered flux

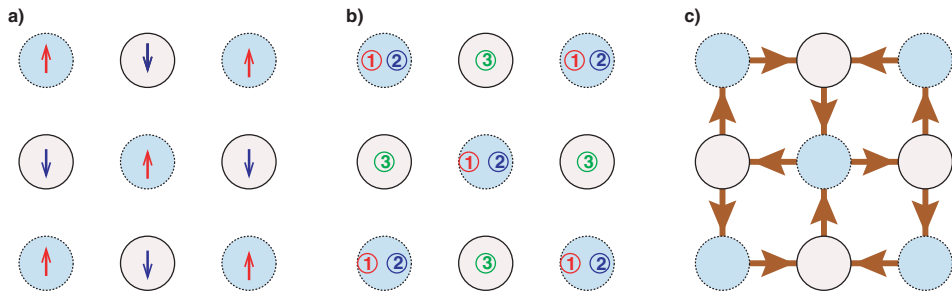


Figure 5. Types of order in the $U > 0$ fermionic $SU(3)$ Hubbard model. (a) AF spin-density wave for $N=2$. (b) Flavor-density wave state for $N=3$. Flavor 1 and 2 prefer one sublattice, flavor 3 the other. (c) Staggered flux state for $N > 6$: particle currents are indicated by arrows. Figures taken from [39].

order, like d -wave superconductivity away from half filling, requires significantly lower temperatures, with a typical RG estimate given by $T_c \approx 0.01 t$ for $N=7$. This is about an order of magnitude below the current experimental limit and will require improved cooling techniques.

Next, we focus on the situation with attractive interactions $U < 0$ and $N=3$ flavors which is relevant for Li^6 . Recently a large experimental effort has been devoted to the BEC–BCS crossover in spin-1/2 superfluid fermions [12–15, 43]. A common feature of these experiments with K^{40} and Li^6 is the use of a Feshbach resonance to generate large attractive interaction and thus achieve Cooper pairing. These resonances generally occur only between two hyperfine spin states and thus cannot be used to realize an $\text{SU}(3)$ symmetric model. However, as pointed out above, Li^6 has a remarkably large and negative background scattering length which in a finite magnetic field, is approximately equal for the three spin states with $m_s = 1/2$. In combination with an optical lattice one can therefore realize the $\text{SU}(N)$ Hubbard model (11) with $U < 0$ and $N=3$. The possibility of a three-flavor paired state in Li^6 , without consideration of the $\text{SU}(3)$ symmetry, had already been pointed out by Modawi and Leggett [44].

Following the analysis in [40] we now discuss how the spin-1/2 BCS state is generalized to three flavors. We assume weak-to-intermediate interactions so that a treatment within BCS theory is qualitatively valid. We introduce a pairing mean-field and Hamiltonian

$$\Delta_{\alpha\beta} = -\frac{U}{N} \sum_{\mathbf{k}} \langle c_{\mathbf{k}\alpha} c_{-\mathbf{k}\beta} \rangle \quad H_{\text{MF}} = -\frac{1}{2} \sum_{\vec{k}, \alpha, \beta} c_{\vec{k}\alpha}^\dagger c_{-\vec{k}\beta}^\dagger \Delta_{\beta\alpha} + h.c., \quad (12)$$

where $\alpha, \beta = 1, \dots, 3$ are the flavor indices and N is the number of lattice sites. We focus on s -wave pairing which is favorable because of strong onsite attraction. The Pauli principle then requires antisymmetry $\Delta_{\alpha\beta} = -\Delta_{\beta\alpha}$ in the flavor index. From a group-theoretical point of view, the flavors $(c_{\mathbf{k}1}, c_{\mathbf{k}2}, c_{\mathbf{k}3})$ transform under a 3-dimensional (3D) irreducible representation of $\text{SU}(3)$, and a Cooper pair $\Delta_{\alpha\beta}$ therefore transforms under $3 \otimes 3 = \bar{3} \oplus 6$. Here $\bar{3}$, which describes the even-parity sector, denotes the complex conjugate representation of 3. The representation 6 is relevant for odd parity pairing (e.g. p -wave) which is not considered here. The order parameter can therefore be written as a triplet

$$\Delta_\alpha = \frac{1}{2} \epsilon_{\alpha\beta\gamma} \langle c_\beta c_\gamma \rangle = \begin{pmatrix} \Delta_{23} \\ -\Delta_{13} \\ \Delta_{12} \end{pmatrix}. \quad (13)$$

From mean-field theory we obtain that all ground states consistent with $\Sigma_\alpha |\Delta_\alpha|^2 = \Delta_0^2$ are degenerate. This 5D ground-state manifold is consistent with the number of collective modes obtained via Goldstones theorem, which is obvious in the gauge $\Delta_{12} = \Delta_0$ and $\Delta_{13} = \Delta_{23} = 0$. The original symmetry group of the problem is $\text{SU}(3) \otimes \text{U}(1)$ – with the extra $\text{U}(1)$ from total particle number conservation – and has nine generators. This gets broken down to an $\text{SU}(2)$ symmetry in flavor 1 and 2, leaving Δ_{12} invariant, and an additional $\text{U}(1)$ that acts on the phase of the unpaired flavor 3. This leaves 5 generators broken, yielding the correct number of Goldstone modes.

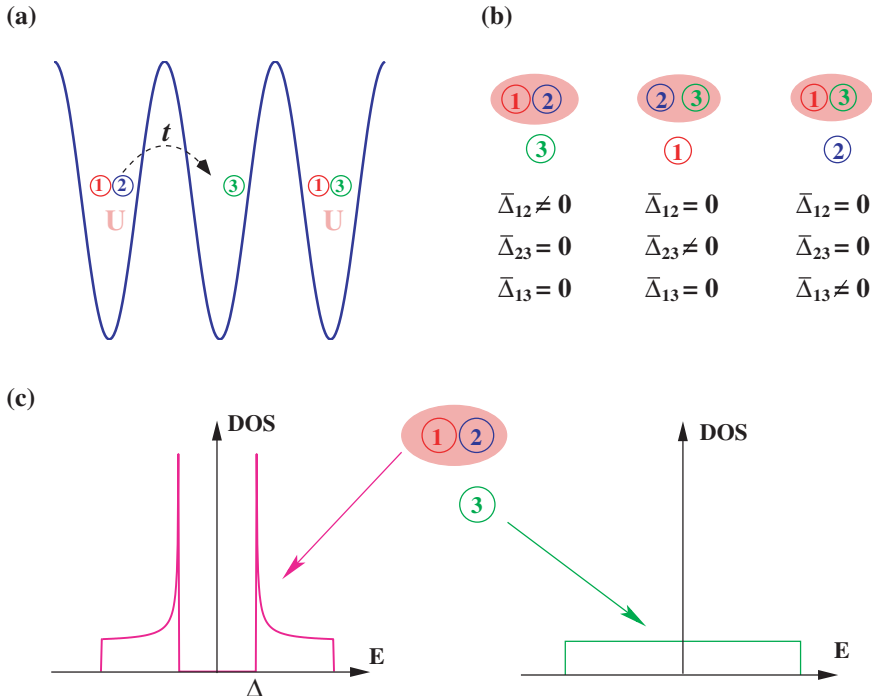


Figure 6. BCS pairing of 3-flavor fermions with SU(3) symmetry: Note that one flavor remains unpaired, with a normal Fermi surface. Figures taken from [40].

The remarkable feature of this triplet s -wave state is that superfluid Cooper pairs coexist with a normal Fermi surface (see figure 6), i.e. the single-particle spectrum is only partially gapped. This has consequences for the collective mode spectrum which we have analyzed within a generalized RPA scheme [40]. They are partially visible in the dynamical structure factor $S(q, \omega)$, which is accessible via Bragg scattering [28]. An example of the calculated density response spectrum $\text{Im}\chi^{\rho}(q, \omega)$, which is equivalent to $S(q, \omega)$ via the fluctuation–dissipation theorem, is shown in figure 7. The Anderson–Bogoliubov mode, the signature of superfluidity, is clearly visible, as well as an additional flavor mode indicating the 3-flavor degeneracy.

From BCS mean-field theory in two dimensions we find a transition temperature of $T_c = 0.17t$ for typical parameters $n = 3/8$ and $U = -4t$. This amounts to roughly $0.05T_F$ and is within reach of present cooling techniques. Multi-component Fermi systems like Li^6 can thus provide exotic new many-body physics and may even allow quantum simulations of simplified QCD models where only the color degree of freedom is taken into account.

4. Disorder and interaction

So far in this review we have focussed on pure, translationally invariant quantum lattice models. It is indeed needed, one of the main advantages of optical lattices that

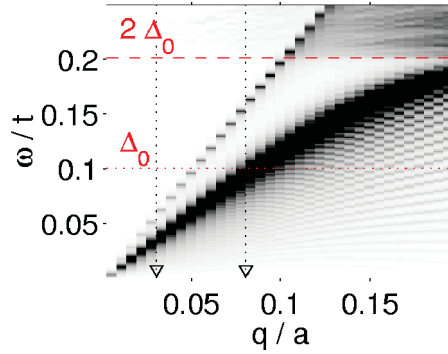


Figure 7. Density response spectrum $\chi^\rho(q, \omega)$ of the 2d fermionic SU(3) Hubbard model at $T=0.01t$, $U=-4t$ and filling $n \approx 0.55$. Figure taken from [40].

perfectly disorder-free systems can be realized. On the other hand, effects of impurities and defects are of central importance in solids, where they often compete with the electron–electron interaction [45, 46]. It is therefore of great interest to realize in a controlled way disordered cold atom systems where localization effects can be studied.

Experimentally, disordered potentials can be created either by using speckle lasers [47] or via quasiperiodic optical lattices [48]. Either way, due to the AC stark effect, the atoms experience a spatially fluctuating random potential which is stationary in time. Recently, localization effects have been observed in a BEC subject to a speckle laser field [49].

Here we focus on *fermionic* atoms with two spin states in a 3D optical lattice with an additional random potential. A complete presentation of the results discussed here can be found in [50]. The system is modelled by the Anderson–Hubbard Hamiltonian

$$H_{\text{AH}} = -t \sum_{\langle ij \rangle \sigma} c_{i\sigma}^\dagger c_{j\sigma} + \sum_{i\sigma} \epsilon_i n_{i\sigma} + U \sum_i n_{i\uparrow} n_{i\downarrow} - \mu \sum_{i\sigma} n_{i\sigma}, \quad (14)$$

where ϵ_i is a random onsite potential which we assume to be uniformly distributed in the interval $[-\Delta/2, \Delta/2]$. The parameter Δ is a measure of the disorder strength. We focus on the case of half filling $n=1$ where on average there is one particle per site. The Hamiltonian (14) describes both an interaction-induced Mott transition into a correlated insulator [51] as well as the Anderson localization transition due to coherent backscattering from random impurities [52].

Analyzing model (14) is a challenging problem. Note that even the pure fermionic Hubbard model with $\Delta=0$ has only been exactly solved in one dimension, while there are many open questions about the physics in two and three dimensions. Here we present results obtained within the *Dynamical Mean-Field Theory* (DMFT), a nonperturbative technique where local quantum fluctuations are treated exactly [53, 54]. The DMFT has been applied with great success in $d=3$ spatial dimensions to explain the magnetic-ordering phenomena and the Mott transition.

In the calculation presented here [50] we use a recently developed variant, the *stochastic* DMFT, which is able to describe Anderson localization as well [55, 56].

Within DMFT, the correlated lattice model is mapped onto a self-consistent Anderson impurity Hamiltonian

$$\begin{aligned}
 H_{\text{SIAM}} = & \sum_{\sigma} (\epsilon - \mu) c_{\sigma}^{\dagger} c_{\sigma} + U n_{\uparrow} n_{\downarrow} \\
 & + \sum_{\mathbf{k}\sigma} V_{\mathbf{k}} c_{\sigma}^{\dagger} a_{\mathbf{k}\sigma} + V_{\mathbf{k}}^{*} a_{\mathbf{k}\sigma}^{\dagger} c_{\sigma} + \sum_{\mathbf{k}\sigma} \epsilon_{\mathbf{k}} a_{\mathbf{k}\sigma}^{\dagger} a_{\mathbf{k}\sigma}
 \end{aligned}
 \tag{15}$$

where a single correlated lattice site now constitutes the impurity with a random onsite energy ϵ , and the fermions $a_{\mathbf{k}\sigma}$ represent a fictitious conduction band with parameters $V_{\mathbf{k}}$ and $\epsilon_{\mathbf{k}}$ which have to be determined self-consistently. The chemical potential $\mu = -U/2$ ensures half filling. This effective single-impurity model is solved using Wilson’s numerical renormalization group [57–60]. Within the stochastic DMFT [56] the self-consistency loop involves a geometric disorder average of the local density of states

$$\rho_{\text{geom}}(\omega) = \exp[\langle \ln \rho_i(\omega) \rangle]
 \tag{16}$$

which then determines the hybridization function $\eta(\omega) = \Sigma_{\mathbf{k}} |V_{\mathbf{k}}|^2 / (\omega - \epsilon_{\mathbf{k}})$ for the next iteration. For more details see [50].

The resulting zero-temperature phase diagram as a function of disorder Δ and interaction U is shown in figure 8. For weak interaction and disorder and atoms are in a Fermi liquid state (‘metal’). There are two different metal insulator transitions: a Mott–Hubbard transition takes place for increasing interaction U , and an Anderson localization transition occurs as a function of Δ . Our results indicate that the two insulating phases are adiabatically connected. Note, however, that in our DMFT calculation we have so far considered only the paramagnetic insulating phase. For non-frustrated lattices (e.g. simple cubic), it is known that an antiferromagnetic instability occurs in the pure Mott state. We are currently analyzing how far this

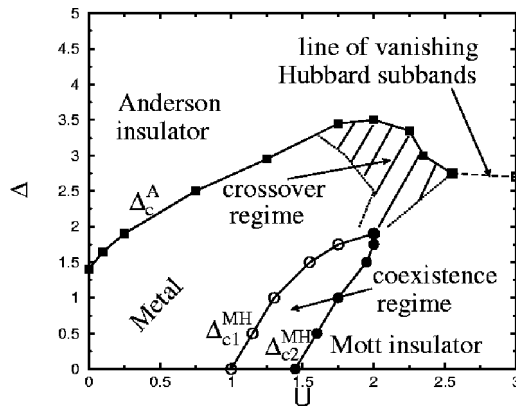


Figure 8. DMFT ground-state phase diagram of the disordered Hubbard model in the nonmagnetic phase at half filling. Figure taken from [50].

antiferromagnetic phase extends into the disordered Mott–Anderson insulator [61]. Let us briefly comment on the detection of these different phases. Itinerant versus insulating behaviour can be identified by a time-flight measurement as in [18]. In the Fermi liquid state, delocalization of fermions across the lattice leads to an interference pattern which vanishes once the atoms become localized. In order to distinguish the antiferromagnetic Mott insulator from the paramagnetic Anderson insulator one could apply spin-resolved Bragg scattering.

Optical lattices are a promising tool to simulate the above phase diagram experimentally since, in contrast to solids, both parameters U and Δ can be tuned arbitrarily. In particular, measurements could be done both in two and three spatial dimensions, thus possibly detecting qualitatively new physics in $d=2$ where DMFT is no longer expected to be a good approximation.

5. Summary and outlook

In this review we have presented some theoretical aspects of strongly correlated atoms in optical lattices. We have shown that these systems can be used to create analogues of well established solid-state quantum phases, like a BCS superconductor, but with much higher tunability of the model parameters. More generally, ultracold atoms can be used to perform quantum simulations of model Hamiltonians, like the 2d Hubbard model, which have not been fully understood theoretically, but may be relevant for fundamental phenomena like high-temperature superconductivity. As another example for such a simulation we have discussed interacting fermions with disorder. Within a DMFT calculation we observe remarkable re-entrance into the itinerant phase due to competing Mott- and Anderson-localization. We expect our results to be qualitatively accurate in 3d, but to which degree the physics carries over to 2d has to be checked experimentally. Finally, we have demonstrated that it is possible to use the highly degenerate internal states of cold atoms to create new exotic quantum states which have no analogue in condensed matter physics. Bosons with multiple spin states can be used to create tunable spin Hamiltonians. Most prominently, we have discussed a new fermionic SU(3) triplet superfluid state which could be relevant for QCD toy models at weak to intermediate interactions. Experimental realization of these quantum phases is within reach and could significantly increase our understanding of the many-body model systems involved.

Acknowledgements

The author would like to thank E. Altman, B. Byczuk, I. Cirac, E. Demler, C. Honerkamp, M.D. Lukin, D. Vollhardt, and P. Zoller for collaborations, and M. Zwierlein and W. Ketterle for discussions on this topic.

References

- [1] M.H. Anderson, J.R. Ensher, M.R. Matthews, *et al.*, Science **269** 198 (1995).
- [2] BEC, for a review see special issue of Nature **416** 206 (2002).

- [3] K.B. Davis, M.-O. Mewes, M.R. Andrews, *et al.*, Phys. Rev. Lett. **75** 3969 (1995).
- [4] B. DeMarco and D.S. Jin, Science **285** 1703 (1999).
- [5] Z. Hadzibabic, C.A. Stan, K. Dieckmann, *et al.*, Phys. Rev. Lett. **88** 160401 (2002).
- [6] F. Schreck, L. Khaykovich, K.L. Corwin, *et al.*, Phys. Rev. Lett. **87** 80403 (2001).
- [7] A.G. Truscott, K.E. Strecker, W.I. McAlexander, *et al.*, Science **291** 2570 (2001).
- [8] S. Inouye, M.R. Andrews, J. Stenger, *et al.*, Nature **392** 151 (1998).
- [9] E. Timmermans, K. Furuyab, P.W. Milonnia, *et al.*, Phys. Lett. A **285** 228 (2001).
- [10] M. Holland, S. Kokkelmans, M.L. Chiofalo, *et al.*, Phys. Rev. Lett. **87** 120406 (2001).
- [11] Y. Ohashi and A. Griffin, Phys. Rev. A **67** 033603 (2003).
- [12] M. Bartenstein, A. Altmeyer, S. Riedl, *et al.*, Phys. Rev. Lett. **92** 120401 (2004).
- [13] C.A. Regal, M. Greiner and D.S. Jin, Phys. Rev. Lett. **92** 04040 (2004).
- [14] M.W. Zwierlein, C.A. Stan, C.H. Schunck, *et al.*, Phys. Rev. Lett. **92** 120403 (2004a).
- [15] M. Greiner, O. Mandel, T. Esslinger, *et al.*, Nature (London) **415** 39 (2002).
- [16] D. Jaksch, C. Bruder, J.I. Cirac, *et al.*, Phys. Rev. Lett. **81** 3108 (1998).
- [17] C. Orzel, A.K. Tuchman, M.L. Fenselau, *et al.*, Science **291** 2386 (2001).
- [18] M. Köhl, H. Moritz, Th. Stöferle, *et al.*, Phys. Rev. Lett. **94** 080403 (2005).
- [19] W. Hofstetter, J.I. Cirac, P. Zoller, *et al.*, Phys. Rev. Lett. **89** 220407 (2002).
- [20] B. Paredes, A. Widera, V. Murg, *et al.*, Nature **429** 277 (2004).
- [21] Th. Stöferle, H. Moritz, Ch. Schori, *et al.*, Phys. Rev. Lett. **92** 130403 (2004).
- [22] C. Kollath, U. Schollwöck, J. von Delft, *et al.*, PRA **69** 031601(R) (2004a).
- [23] C. Kollath, U. Schollwöck, J. von Delft, *et al.*, preprint cond-mat/0411403 (2004).
- [24] M.C. Gutzwiller, Phys. Rev. Lett. **10** 159 (1963).
- [25] J. Hubbard, Proc. Roy. Soc. London A **276** 238 (1963).
- [26] J. Kanamori, Prog. Theor. Phys. **30** 275 (1963).
- [27] R. Micnas, J. Ranninger and S. Robaszkiewicz, Rev. Mod. Phys. **62** 113 (1990).
- [28] D. Stamper-Kurn and W. Ketterle, *Spinor Condensates and Light Scattering from Bose-Einstein Condensates*, Les Houches lecture notes and cond-mat/0005001 (1999).
- [29] J. Steinhauer, R. Ozeri, N. Katz, *et al.*, Phys. Rev. Lett. **88** 120407 (2002).
- [30] R. Feynman, Int. J. Theor. Phys. **21** 467 (1982).
- [31] D.M. Stamper-Kurn, M.R. Andrews, A.P. Chikkatur, *et al.*, Phys. Rev. Lett. **80** 2027 (1998).
- [32] O. Mandel, M. Greiner, A. Widera, *et al.*, Phys. Rev. Lett. **91** 010407 (2003).
- [33] E. Altman, W. Hofstetter, E. Demler, *et al.*, New J. Phys. **5** 113.1 (2003).
- [34] L.-M. Duan, E. Demler and M.D. Lukin, Phys. Rev. Lett. **91** 090402 (2003).
- [35] K. Sheshadri, H.R. Krishnamurthy, R. Pandit, *et al.*, Europhys. Lett. **22** 257 (1993).
- [36] E. Altman, E. Demler and M.D. Lukin, Phys. Rev. A **70** 013603 (2004).
- [37] C.A. Regal and D.S. Jin, Phys. Rev. Lett. **90** 230404 (2003).
- [38] E.R.I. Abraham, W.I. McAlexander, J.M. Gerton, *et al.*, Phys. Rev. A **55** R3299 (1997).
- [39] C. Honerkamp and W. Hofstetter, Phys. Rev. Lett. **92** 170403 (2004a).
- [40] C. Honerkamp and W. Hofstetter, Phys. Rev. B **70** 094521 (2004b).
- [41] J.B. Marston and I. Affleck, Phys. Rev. B **39** 11538 (1989).
- [42] C. Honerkamp and M. Salmhofer, Phys. Rev. B **64** 184516 (2001); Phys. Rev. Lett. **87** 187004.
- [43] M.W. Zwierlein, C.H. Schunck, C.A. Stan, *et al.*, Phys. Rev. Lett. **94** 180401 (2005).
- [44] A.G.K. Modawi and A.J. Leggett, J. Low Temp. Phys. **109** 625 (1997).
- [45] D. Belitz and T.R. Kirkpatrick, Rev. Mod. Phys. **66** 261 (1994).
- [46] P.A. Lee and T.V. Ramakrishnan, Rev. Mod. Phys. **57** 287 (1985).
- [47] P. Horak, J.Y. Courtois and G. Grynberg, Phys. Rev. A **58** 3953 (1998).
- [48] L. Guidoni, C. Triché, P. Verkerk, *et al.*, Phys. Rev. Lett. **79** 3363 (1997).
- [49] J.E. Lye, L. Fallani, M. Modugno, *et al.*, cond-mat/0412167 (2004).
- [50] K. Byczuk, W. Hofstetter and D. Vollhardt, Phys. Rev. Lett. **94** 056404 (2005).
- [51] N.F. Mott, Proc. Phys. Soc. A **62** 416 (1949).
- [52] P.W. Anderson, Phys. Rev. **109** 1492 (1958).
- [53] A. Georges, G. Kotliar, W. Krauth, *et al.*, Rev. Mod. Phys. **68** 13 (1996).
- [54] W. Metzner and D. Vollhardt, Phys. Rev. Lett. **62** 324 (1989).
- [55] V. Dobrosavljević and G. Kotliar, Phys. Rev. Lett. **78** 3943 (1997).

- [56] V. Dobrosavljević, A.A. Pastor and B.K. Nikolić, *Europhys. Lett.* **62** 76 (2003).
- [57] R. Bulla, A.C. Hewson and Th. Pruschke, *J. Phys.: Condens. Matter* **10** 8365 (1998).
- [58] T.A. Costi, A.C. Hewson and V. Zlati, *J. Phys.: Cond. Mat.* **6** 2519 (1994).
- [59] W. Hofstetter, *Phys. Rev. Lett.* **85** 1508 (2000).
- [60] K.G. Wilson, *Rev. Mod. Phys.* **47** 773 (1975).
- [61] K. Byczuk, W. Hofstetter and D. Vollhardt, in preparation (2005).